

# Scale Effects on the Reproducibility of Morphological Parameters of Natural Sand by 3D Printing

Anusree KV<sup>1</sup> and Gali Madhavi Latha<sup>2</sup>[0000-0002-9910-5624]

<sup>1</sup> PhD Candidate, Dept. of Civil Engineering, Indian Institute of Science, Bangalore, India

<sup>2</sup> Professor, Dept. of Civil Engineering, Indian Institute of Science, Bangalore, India  
lncs@springer.com

**Abstract.** The study of individual effects of morphological properties of sand grains, such as their size, shape, and surface roughness, is of great importance while dealing with problems of liquefaction and cyclic mobility, as these microscopic characteristics significantly influence the physical, mechanical and hydraulic behaviour of sands. 3D printed granular media with representative morphological characteristics of natural sand grains enable us to control particle size and shape, thus permitting a comprehensive investigation of the effect of individual parameters. This study aims to critically evaluate the capability of 3D printed media reproduced at different scales to capture the morphological characteristics of natural sands through a well-established image analysis method. A completely automated image analysis procedure characterizes the 2D morphology indices of 3D printed media and natural sands. The effect of the scale of reproduction of the 3D printed materials and other critical parameters on the reproducibility of morphological characteristics of the original medium is assessed through an analytical comparison of these indices.

**Keywords:** Morphological Characterization, 3D Printing, Image Analysis, Granular Material

## 1 Introduction

The morphological properties of grains, such as size, shape, and surface roughness, are critical parameters that considerably influence the physical, mechanical, and hydraulic behavior of sands [1, 2]. Critical insight into the characterization of morphological parameters and their influence on macro scale response of sand like compressibility, permeability, response to shear loading etc., will help in a more judicial and efficient utilization of this geomaterial.

Method of characterization of size and shape has evolved from sieving and visual inspection and comparison to standard charts [3, 4] to 2D and 3D image acquisition and analysis in the recent past [5, 6]. Various methods have been proposed to quantify the size and shape parameters of grains through the analysis of two-dimensional images captured using SEM, high-resolution cameras etc. [6, 7]. Utilization of these advanced image capture systems and robust algorithms have been used to accurately predict the morphological parameters such as dimensions of the grains, sphericity, roundness, angularity etc.

The effect of micro-scale properties of grains on the macro-scale response of sand, while being of critical significance, has seldom been studied systematically. Experimental investigation into the effect of different morphological parameters, aided with numerical simulations, essentially requires decoupling the effect of one parameter from another, apart from the accurate characterization of these parameters. While different tools are available for determining the size and morphology of grains, it is extremely difficult to control the parameters in natural geomaterials. It is in this context that the advancements in 3D printing technology have become significant. It has been shown that 3D-printed granular media that possess the shape parameters of natural granular materials or with desired shape parameters can be manufactured efficiently to conduct experimental studies [8, 9].

An appropriate choice of printing mechanism is important while carrying out 3D printing to recreate the shape of granular media. This paper focuses on the effects of the scale of printing, as well as different printing mechanisms, on the reproducibility of the desired shape of 3D printed materials. 2D image analysis is carried out on 3D printed materials to assess the shape of the same. Obtained results are compared with that of the original grain of sand that served as the reference material for 3D printing. The reproducibility of the reference material using the 3D printing mechanism is discussed.

## 2 3D printing of granular material

3D-printed granular materials were printed using two different printing technologies from the Standard Tessellation Language (STL) file of a natural sand grain. The dimensions of the reference sand grain were 7.07 mm × 5.802 mm × 3.602 mm. Two printers with different printing technologies were used in this study. Particles were printed using both these printers and the ability of the printers in accurately reproducing the morphological properties of the grain were compared. The first printer used was a Digital Light Processing (DLP) printer with a photopolymer base and a printing resolution of 63 μm in the X and Y axes and 10-50 μm in the Z axis, while the second one was a Stereolithography (SLA) printer with photopolymer resin base and a resolution of 25 μm in the XY direction.

The DLP printer was used to print granular particles at scales of 0.6 and 4, and the SLA printer was used to print the particles at scales of 1.98, 4 and 7.07. The sizes of the 3D printed particles were 4.243 mm × 3.481 mm × 2.161 mm at the scale of 0.6, 14 mm × 11.49 mm × 7.13 mm at the scale of 1.98, 28.287 mm × 23.209 mm × 14.409 mm at the scale of 4 and 50 mm × 41.026 mm × 25.471 mm at the scale of 7.07. The scales were chosen to facilitate the printing of particles with minimum dimensions without losing many details. The smallest scales from both printers corresponded to the least dimensions that could be achieved without incorporating texture, while the largest from each printer corresponded to the least dimensions that were possible if the texture was also incorporated. The analysis of printed grains thus will aid in the selection of the best printing mechanism as well as the suitable scale of printing. The 3D printed particle at different scales is shown in Fig. 1.

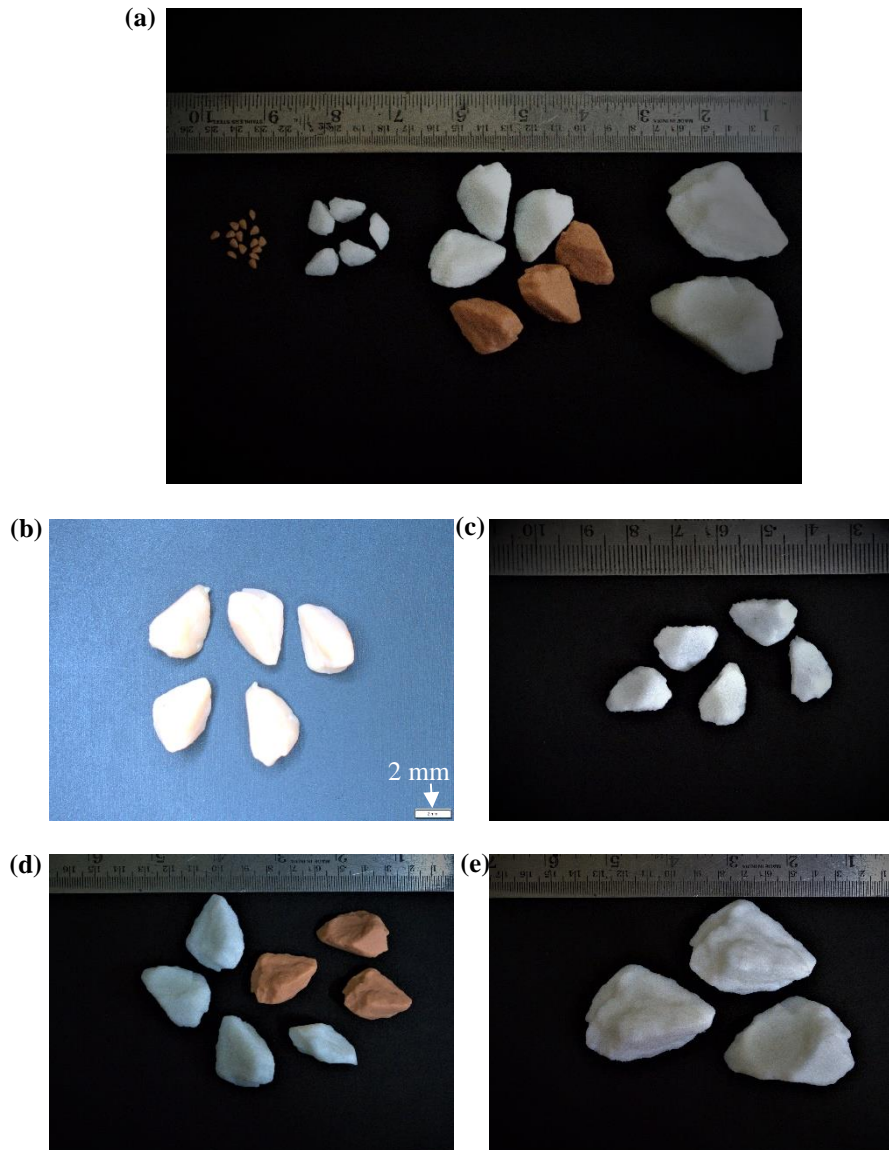


**Fig. 1.** Photographs of 3D printed particles (a) 3D printed particles at four different scales, (b) particles printed at the scale of 0.6 (PA), (c) 1.98 (PB), (d) 4 (PC -White and PD – Orange), (e) 7.07 (PE)

### 3 Image analysis of 3D printed particles

The size and shape of grains have been described using several parameters in the literature [10, 11]. However, it is important to choose the minimum number of parameters that will give an accurate representation of the particle and are independent of each other. Form, roundness, and surface texture have been identified as the independent parameters of particle shape [11]. Form represents the overall proportions of the particle; roundness represents the sharpness of particle corners and surface texture describes the fine details superimposed on form and roundness. The variations in one of these parameters do not result in the variations in the other two, and hence they are independent parameters.

Various definitions have been proposed for form and roundness. Among those, Wadell's definition of roundness [10] has prevailed over time. In this paper, Wadell's roundness and width-to-length ratio sphericity [3] are used to characterize particle shape. Since the 3D printing mechanism is not equipped to capture the fine roughness details of grains, surface roughness is not considered. The length, width, and area of the grains are used to quantify the particle size. The method of obtaining these parameters through image analysis is described in the subsequent sections.

#### 3.1 2D image analysis procedure

An algorithm was written and developed in MATLAB according to the method proposed by [7] for 2D image analysis of granular materials. A brief description of the procedure is given below.

**Image filtering.** In order to accurately quantify the form and roundness of the particles, it is necessary to remove the noise, as well as the surface roughness features imposed on the particle morphology. This is done through filtering in the frequency domain. The captured image is first binarized into a binary image using the MATLAB function *imbinarize*, followed by which the boundary of the binary image is traced at a constant interval of 0.1 degrees from the centroid of the particle in the clockwise direction. The traced boundary is converted into the frequency domain from the spatial domain to aid in filtering using the Fast Fourier Transform (FFT) algorithm in MATLAB. A Gaussian regression filter [13] was used to filter out the noise and roughness at specified cutoff frequencies. The Gaussian regression filter has a superior performance over a conventional Gaussian filter. Filtering is carried out by reducing the departure of the raw profile segment from a second-order polynomial to obtain the mean line component at each point of the profile. Fig. 2 shows the unfiltered and filtered boundary profiles of an image of a particle adopted from [13]. The filtered boundary profile is free of noise and roughness, which is essential for carrying out roundness computations. The image is reconstructed from the filtered boundary coordinates after taking the inverse Fourier transform.

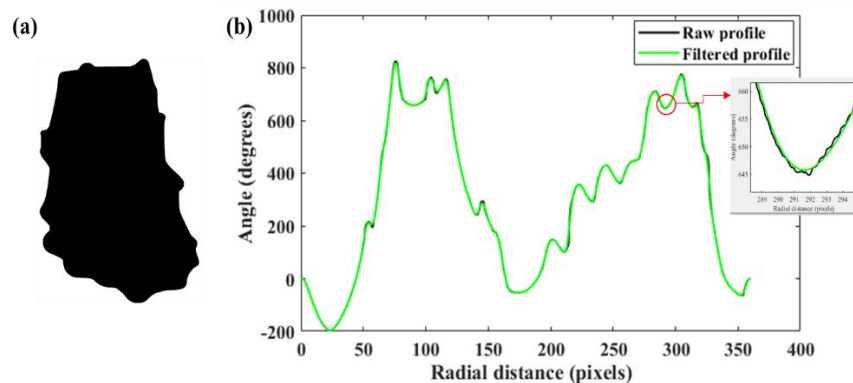


**Fig. 2.** Filtering of roughness (a) Silhouette of a sand particle adopted from Powers [13], (b) Raw profile and roughness filtered profile of the particle

**Detection of dominant points.** The details of the particle boundary can be described using a few key points called dominant points. Dominant points are detected using a linear polygonal approximation method [7]. As the first step, points A and B are located on the particle boundary such that the length AB represents the maximum distance between any two points on the boundary. Next, points C and D are located on opposite sides of AB, at maximum perpendicular distances from AB. Similarly, E, F, G, and H are found using vectors AC, CB, BD, and DA. The procedure is repeated until the maximum perpendicular distance from a vector to any boundary point does not exceed a threshold value of  $n$  (see Fig. 3).

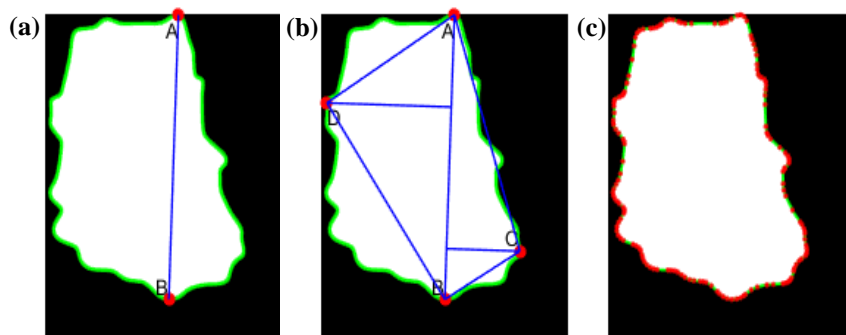


**Fig. 3.** Steps in dominant point detection (a) Location of initial points A and B (b) Points C and D after the first iteration (c) Detected dominant points after the final iteration

**Detection of corners.** Wadell [10] defines corners as ‘every such part of the outline of an area (projection area) which has a radius of curvature equal to or less than the radius of curvature of the maximum inscribed circle of the same area’. All sets of three points which are concave inwards were identified to detect the corners. Then the continuity of these three-point sets was evaluated, and sets of points which formed continuous corner regions were identified. Next, inflexion points were identified to separate potential continuous corner regions in which two corners of different curvatures are linked together by a flat region and will essentially appear as a concave inwards region. The rate of change of slope at every corner point was calculated using a modified double derivative formula, and points with a rate of change of slope less than a threshold value were identified as inflexion points. The steps are shown in Fig. 4.

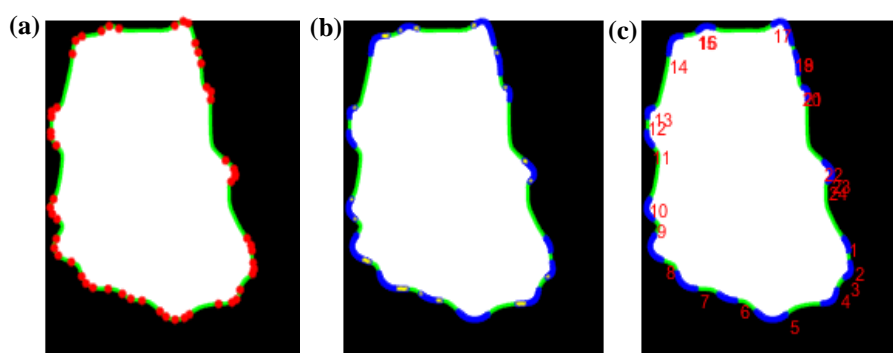


**Fig. 4.** Steps in corner detection (a) Start and end points of all three-point corner regions B (b) Potential continuous corner regions (in blue) with inflexion points detected (in yellow), (c) Final corner regions.

**Finding the best-fitting circle at each corner.** In order to calculate the roundness, the best-fitting circle in each corner must be determined. Firstly, the radius of curvature and centre of curvature of each point in the corner is calculated. Since the radius of curvature of each corner should be less than the radius of the maximum inscribed circle according to Wadell’s definition, all such circles are eliminated (Step 1). For this, the maximum inscribed circle is found by using the distance transformation algorithm. The minimum distance to the nearest boundary pixel is calculated for the binary image, and the maximum of these distances becomes the radius of the maximum inscribed circle. Following this, all circles going out of the particle boundary are removed (Step 2), and then circles which are not tangential to the stationary point are removed (Step 3). Finally, the best-fitting circle is found to be the one which is tangential to the maximum number of dominant points in the corner (Step 4). Corners which are left with no circles are removed. Fig. 5 demonstrates these steps.

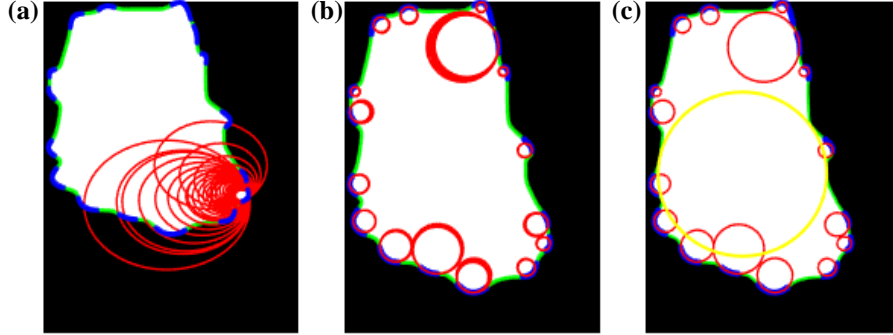


**Fig. 5.** Steps in finding best fitting circles in corners (a) Circles remaining at corner 2 after step 1 (b) Circles remaining at every corner after steps 3 and 4 (c) Best fitting circle at every corner and maximum inscribed circle (in yellow)

**Length, Width, and Area of the particle.** The length of the particle,  $L$ , is the length of the main axis as found from the polygon approximation method (length AB). The width of the particle,  $W$ , is found by locating points at maximum distance from AB on either side of AB. The sum of these perpendicular distances is defined as the width of the particle. The area of the particle is found using the *regionprops* function in MATLAB.

**Sphericity of the particle.** Sphericity is computed as the ratio of width to length of the particle.

**Roundness of the particle.** Roundness is computed as per Wadell's definition, using Eqn. 1.

$$R = \frac{\sum_{r=1}^n D_r}{D_i} \quad (1)$$

Where  $D_r$  is the diameter of the  $r^{\text{th}}$  circle,  $n$  is the total number of circles, and  $D_i$  is the diameter of the maximum inscribed circle.

### 3.3 Image acquisition

As the size of particles varied over a wide range, it was necessary to use two different instruments for capturing the images. For the 3D printed particles of scales 0.6 and 1.98, an Olympus Stereo Microscope was used, while for particles printed at scales 4 and 7.07, a High Definition camera was used. The images captured at high magnification ensured that any undesirable effect due to low resolution during image processing was avoided.

Five particles each of scales 0.6 printed with DLP printer (PA) and 1.98 printed with SLA printer (PB), three particles each of scale 4 printed with SLA printer (PC), and DLP printer (PD) and three particles of scale 7.07 printed with SLA printer (PE) were

selected as representative samples. This selection enabled us to study the effect of the printing mechanism and scale of printing separately on the 3D-printed particles of the same shape.

Images of each particle were captured at three different orientations. Three orientations were chosen to bring the analysis as close as possible to a 3D analysis since capturing the image at only one orientation might result in missing important features of the particle morphology. The three orientations chosen were stable positions for the particles. Particle PA at the three different orientations is shown in Fig. 6.



**Fig. 6.** The three orientations at which images were captured (a) Plane 1, (b) Plane 2, and (c) Plane 3, for particle PA

#### 4 Results and discussions

Length, Width, Area, Roundness and Sphericity were calculated for each particle imaged at three different orientations. The length, width and area were normalized with the scale of printing for a more accurate comparison. The mean and standard deviation (SD) of each of the samples were calculated and are presented in subsequent tables.

The morphological parameters of the natural sand grain used as the reference for 3D printing were also obtained through image analysis of projections of the 3D volume in the three different planes. These values would serve as the reference for comparing the respective parameters of the 3D-printed particles. Fig. 7 shows the 2D projections, processed images and obtained morphological parameters of the reference sand grain.

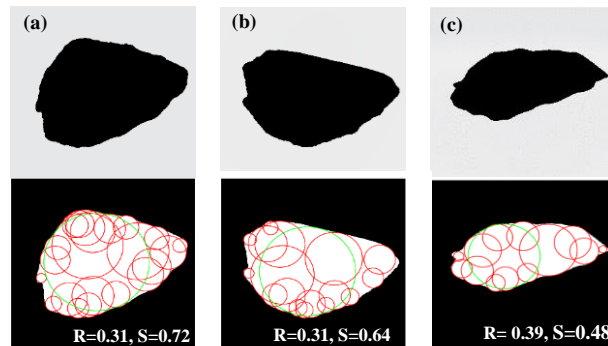


**Fig. 7.** 2D projections, processed images and obtained morphological parameters of the reference sand grain for (a) Plane 1, (b) Plane 2, and (c) Plane 3

#### 4.1 Comparison of shape parameters

The mean value of roundness and the standard deviation for each sample is presented in Table 1. As we can see from the table, the scaled-down Particle A roundness values that are considerably different from that of the reference particle in all three planes. The failure of the printing mechanism to capture fine details of the reference sand grain at a lower scale of printing could be the reason for this. Also, Particle B has a significantly lower value of roundness in planes 1 and 2. The reason could be attributed to rough corrugations present on one face of particle B, which is evident from Fig. 8 (a) and (b). It should also be noted that these irregularities are only noticeable when viewed under a microscope and not during the visual inspection using the naked eye, which underscores the importance of carrying out a proper inspection of the 3D-printed particles. It can be said that the DLP printer at a scale of 0.6 and the SLA printer at a scale of 1.98 fails to recreate the reference morphology. On the contrary, 3D printed particles at scale 4 using both SLA and DLP printers and at scale 7.07 using SLA printer can capture the roundness of the reference particle accurately. The mean value of roundness is comparable to that of the reference particle, and the SD values are comparatively lower. At the scale of 4, the DLP printer has a superior performance over the SLA printer.

**Table 1.** Mean and SD of roundness for each sample

Particle ID	Plane 1		Plane 2		Plane 3	
	Mean	SD	Mean	SD	Mean	SD
PA	0.48	0.03	0.35	0.03	0.34	0.02
PB	0.20	0.03	0.23	0.02	0.36	0.04
PC	0.29	0.01	0.33	0.02	0.36	0.01
PD	0.32	0.01	0.33	0.02	0.38	0.00
PE	0.32	0.01	0.32	0.01	0.38	0.03

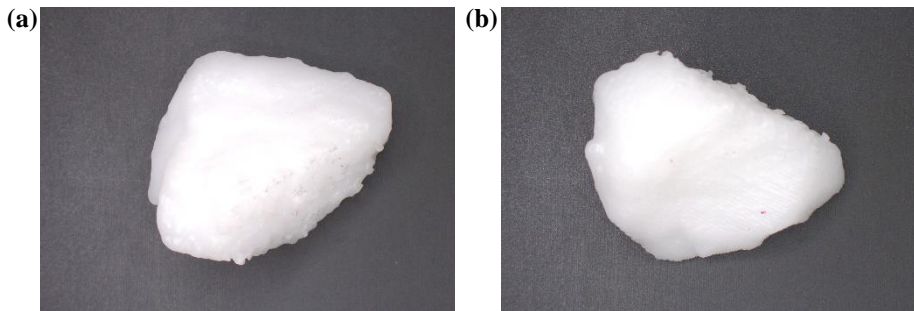


**Fig. 8.** 2D projections for Particle B (a) Plane 1, (b) Plane 2

The mean and SD values for the sphericity of the five samples are given in Table 2. The mean value of sphericity of all samples is comparable to that of the reference

particle in all three planes. The standard deviation values are also negligible, indicating that different particles in the same scale can be reproduced accurately without considerable change in their form. A slight discrepancy can be found for Particle B, which was printed at a scale of 1.98 using the SLA printer. However, both SLA and DLP printers have a satisfactory performance when it comes to the proportions of the particle.

**Table 2.** Mean and SD of sphericity for each sample

Particle ID	Plane 1		Plane 2		Plane 3	
	Mean	SD	Mean	SD	Mean	SD
PA	0.71	0.01	0.65	0.01	0.51	0.00
PB	0.74	0.00	0.69	0.03	0.46	0.00
PC	0.72	0.00	0.65	0.01	0.47	0.00
PD	0.70	0.00	0.64	0.00	0.47	0.00
PE	0.71	0.00	0.66	0.01	0.47	0.00

#### 4.2 Comparison of size parameters

Tables 3, 4, and 5 show the comparison of the normalized length, width and area of each of the 3D-printed samples. It should be noted that deviations in the values of length, width, and area are justified as slight differences in the projection plane are bound to cause comparatively large differences in the size parameters rather than in shape parameters. Even so, a comparison is possible from the values of standard deviations of the samples. As we can see, particles A and B printed at smaller scales of 0.6 and 1.98 have much larger values of SD for both length and projection area. This indicates that the particles printed at the same scale might differ in their dimensions at smaller scales of printing. However, SD values at larger scales of 4 for both the printers and at 7.07 for the SLA printer have considerably lower values of SD for all three parameters in all three planes, proving their ability to reproduce the particles rather accurately.

**Table 3.** Mean and SD of normalized length for each sample

Particle ID	Plane 1		Plane 2		Plane 3	
	Mean	SD	Mean	SD	Mean	SD
PA	7.45	0.04	7.57	0.07	7.58	0.07
PB	7.70	0.03	7.57	0.11	7.68	0.06
PC	7.78	0.02	7.45	0.01	7.81	0.01
PD	7.27	0.03	6.99	0.03	7.31	0.01
PE	7.55	0.04	7.11	0.05	7.51	0.01

**Table 4.** Mean and SD of normalized width for each sample

Particle ID	Plane 1		Plane 2		Plane 3	
	Mean	SD	Mean	SD	MEAN	SD
PA	5.29	0.03	4.91	0.05	3.85	0.05
PB	5.65	0.05	5.24	0.14	3.56	0.03
PC	5.55	0.01	4.85	0.08	3.69	0.01
PD	5.08	0.00	4.48	0.04	3.46	0.01
PE	5.34	0.01	4.62	0.01	3.57	0.01

**Table 5.** Mean and SD of normalized area for each sample

Particle ID	Plane 1		Plane 2		Plane 3	
	Mean	SD	Mean	SD	Mean	SD
PA	26.40	0.43	26.20	0.32	19.83	0.36
PB	29.47	0.16	27.89	0.29	18.84	0.19
PC	30.20	0.09	26.39	0.24	19.65	0.04
PD	25.59	0.08	22.65	0.25	17.33	0.01
PE	27.77	0.10	24.09	0.25	18.27	0.04

## 5 Summary and conclusions

This paper validates the reproducibility of morphological parameters of sand particles printed to different scales using 3D printing. A natural sand particle was printed to scales 0.6, 1.98, 4 and 7.07 using DLP and SLA 3D printing techniques. Size parameters length, width, and area and shape parameters roundness and sphericity of the 3D printed particles are compared with those of the reference particle.

3D printed particles at scales of 4 by both DLP and SLA printers and at scale 7.07 by SLA printer have roundness values comparable to that of the reference particle, while particles printed at lower scales of 0.6 and 1.98 failed to reproduce the reference roundness values. The sphericity at all four scales of printing and using both printers have mean values closer to that of the reference sphericity value. However, particles printed at larger scales have better reproductions of morphological properties compared to those printed at lower scales of 0.6 and 1.98. While the normalized length, width and area of the 3D printed particles at lower scales showed higher values of standard deviation at scales 4 and 7.07, both the printers reproduced samples with similar dimensions fairly well. Results demonstrated that the morphological properties of the sand particles can be reproduced satisfactorily at scales of 4 or higher, using either DLP or SLA

printers. This study delineates the importance of carrying out a proper investigation into the capability of the 3D printing mechanism to reproduce the desired morphological parameters of the sand grains. However, the mechanical properties of the 3D printed particles may vary significantly with scaling and printing techniques. The comparison of mechanical properties needs further investigation.

## Acknowledgement

The digital microscope and HD camera used for the study were procured through the SERB POWER Fellowship grant. 3D printing of particles is financially supported by SERB Core Research Grant. The authors are grateful to the Department of Science and Technology, India for this support.

## References

1. Mitchell, J. K., Soga, K.: *Fundamentals of soil behaviour*. Vol. 3. John Wiley & Sons, New York (2005).
2. Cho, G.C., Dodds, J., Santamarina, J.C.: Particle shape effects on packing density, stiffness, and strength: natural and crushed sands. *J. Geotech. Geoenviron. Eng.* 5, 591–602 (2006).
3. Krumbein, W.C., Sloss, L.L.: Stratigraphy and sedimentation. *Soil Sci.* 71, 401 (1951).
4. Powers, M.C.: A new roundness scale for sedimentary particles. *J. Sediment. Res.* 23, 117–119 (1953).
5. Fonseca, J., O'sullivan, C., Coop, M. R., Lee, P. D.: Non-invasive characterization of particle morphology of natural sands. *Soils and Foundations* 52(4), 712-722 (2012).
6. Zheng, J., Hryciw, R.D.: Traditional soil particle sphericity, roundness and surface roughness by computational geometry. *Geotechnique* 65, 494–506 (2015).
7. Vangla, P., Roy, N., Gali, M. L.: Image based shape characterization of granular materials and its effect on kinematics of particle motion. *Granular Matter* 20(1), 1-19 (2018).
8. Ahmed, S. S., Martinez, A.: Triaxial compression behavior of 3D printed and natural sands. *Granular Matter* 23(4), 1-21 (2021).
9. Adamidis, O., Alber, S., Anastasopoulos, I.: Assessment of three-dimensional printing of granular media for geotechnical applications. *Geotechnical Testing Journal* 43(3), (2019).
10. Wadell, H.: Sphericity and roundness of rock particles. *J. Geol.* 41, 310–331 (1933).
11. Barrett, P.J.: The shape of rock particles, a critical review. *Sedimentology* 27, 291–303 (1980).
12. Raja, J., Muralikrishnan, B., Fu, S.: Recent advances in separation of roughness, waviness and form. *Precis. Eng.* 26, 222–235 (2002).
13. Powers, M.C.: A new roundness scale for sedimentary particles. *J. Sediment. Res.* 23, 117–119 (1953).